ISSN 1674-1056
http://cpb.iphy.ac.cn
http://iopscience.iop.org/cpb
中国物理 B
Chinese Physics
中国物理 Chinese Physics B

Orientation dependence of elastic properties in orthorhombic $Ca_3Mn_2O_7$

Gang Jian(简刚), Mei-Rui Liu(刘美瑞), Chen Zhang(张晨), Jie Lu(卢杰), Chao Yan(晏超)

Citation: Chin. Phys. B . 2019, 28(2): 026201. **doi:** 10.1088/1674-1056/28/2/026201
Journal homepage: http://cpb.iphy.ac.cn; http://iopscience.iop.org/cpb

What follows is a list of articles you may be interested in

Stability, elastic anisotropy, and electronic properties of Ca_2C_3

Quan Zhang(张权), Qun Wei(魏群), Hai-Yan Yan(闫海燕), Xuan-Min Zhu(朱轩民), Jun-Qin Zhang(张军琴), Xiao-Fei Jia(贾晓菲), Rong-Hui Yao(姚荣辉)

Chin. Phys. B . 2017, 26(6): 066201. **doi:** 10.1088/1674-1056/26/6/066201

Elastic properties and electronic structures of lanthanide hexaborides

Duan Jie, Zhou Tong, Zhang Li, Du Ji-Guang, Jiang Gang, Wang Hong-Bin

Chin. Phys. B . 2015, 24(9): 096201. **doi:** 10.1088/1674-1056/24/9/096201

Structural and mechanical stability of rare-earth diborides

Haci Ozisik, Engin Deligoz, Kemal Colakoglu, Gokhan Surucu

Chin. Phys. B . 2013, 22(4): 046202. **doi:** 10.1088/1674-1056/22/4/046202

First-principles study of structural stability and elastic property of pre-perovskite $PbTiO_3$

Liu Yong, Ni Li-Hong, Ren Zhao-Hui, Xu Gang, Li Xiang, Song Chen-Lu, Han Gao-Rong

Chin. Phys. B . 2012, 21(1): 016201. **doi:** 10.1088/1674-1056/21/1/016201

Elastic properties of Nb-based alloys by using the density functional theory

Liu Zeng-Hui, Shang Jia-Xiang

Chin. Phys. B . 2012, 21(1): 016202. **doi:** 10.1088/1674-1056/21/1/016202

Orientation dependence of elastic properties in orthorhombic $Ca_3Mn_2O_7$

Gang Jian(简刚)[1,2,†], Mei-Rui Liu(刘美瑞)[1], Chen Zhang(张晨)[1], Jie Lu(卢杰)[1], and Chao Yan(晏超)[1,‡]

[1] *School of Materials Science and Engineering, Jiangsu University of Science and Technology, Zhenjiang* 212003, *China*
[2] *School of Materials Science and Engineering, Georgia Institute of Technology, Atlanta* 30332, *USA*

(Received 1 October 2018; revised manuscript received 11 December 2018; published online 25 January 2019)

Elastic properties are important in fundamental understanding of multiferroic materials. However, up to now, there is no work about anisotropy of elastic properties in orthorhombic $Ca_3Mn_2O_7$. In this study, using coordinate transformation method, we investigated basic elastic parameters (elastic constants c'_{ij}) and engineering elastic parameters (Young's modulus E', Poisson's ratio ν', and the rigidity modulus G') of orthorhombic $Ca_3Mn_2O_7$ along arbitrary orientations. The detailed anisotropic characteristics of these parameters were presented. The results reveal the orientation related elastic properties in *mm*2 point group orthorhombic $Ca_3Mn_2O_7$.

Keywords: $Ca_3Mn_2O_7$, elastic properties, coordinate transformations, orientation dependence

PACS: 62.20.de, 64.30.Jk, 71.15.Mb, 71.27.+a **DOI:** 10.1088/1674-1056/28/2/026201

1. Introduction

Multiferroic materials with perovskite structures have been widely studied in the past decade, including $BiFeO_3$,[1] $TbMnO_3$,[2] *etc*. for the purpose of exploring possible magnetisms in ferroelectric compounds. Recently, layered perovskites have been actively pursued as multiferroic materials. $Ca_2Mn_2O_7$ is one of the compounds which was first studied for its colossal magnetoresistance effect,[3] and was later proposed to have a hybrid improper ferroelectricity and strong polarization-magnetization couplings.[4] This indicates it could be a good candidate for new magnetoelectric single-phase materials. The chemical formula $Ca_3Mn_2O_7$ also can be written as $CaO(CaMnO_3)_2$ that means a layered perovskite structure with two MnO_6 octahedral layers in the perovskite block.[5] In this ferroelectric $Ca_3Mn_2O_7$, a *G*-type antiferromagnetic order is believed to exist below the Neel temperature of around 112 K.[6] Concerning of crystal symmetry of $Ca_3Mn_2O_7$ at these temperatures, Bendersky *et al.* and Lobanov *et al.* proposed it has a $Cmc2_1$ space group (Hall symbol: *C* 2*c*-2) symmetry,[6,7] while the recent studies show it has an $A2_1am$ space group (Hall symbol: *A*-2 2*a*) symmetry.[8–11] However, both of $Cmc2_1$ and $A2_1am$ are C_{2v}^{12} in Schoenflies symbols and both of them are No. 36 space group, and finally, both of them belong to *mm*2 point group with orthorhombic system.[12,13] Up to now, many efforts have been made to extensively investigate magnetic, electronic, symmetry properties of $Ca_3Mn_2O_7$.[14–17]

Elastic parameters are measurements of mechanical properties of a solid. They are closely related to specific heat, phonon spectrum, and Debye temperature of a solid,[19–21] and thus, they are very important in strain energy investigations. Moreover, elastic properties have decisive effects in magnetoelectric coupling coefficients in multiferroic materials because of the magnetic–mechanical–electric transformations.[22,23] At the atomic scale, the Harshe model can be used for single-phase compounds having strong electromaechanical and megnetomechanical interactions, from which the magnetoelectric coefficients α_{E31} (transverse) and α_{E33} (longitudinal) are both increasing with decreasing $c_{11}+c_{12}$ or with increasing $s_{11}+s_{12}$.[23,24] Elastic parameters include basic parameters as elastic constants and engineering elastic parameters including Young's modulus, Possion's ratio, and the rigidity modulus. Because $Ca_3Mn_2O_7$ has an asymmetrical crystal structure, it is meaningful to have a fundamental understanding of anisotropy of elastic properties. Up to now, there is no work on the detailed anisotropy of elastic parameters in $Ca_3Mn_2O_7$, especially there lacks of numerical results along arbitrary directions. Coordinate transformation is a method proved to be effective in predicting orientation dependences of properties varying with different crystal-symmetries (point groups), including piezoelectric constants of 4*mm* $BaTiO_3$,[25] electromechanical coupling factors of 3*m* $LiNbO_3$ and $LiTaO_3$,[26] and piezomagneitc coefficients of *m*3*m* $NiFe_2O_4$.[27]

In this research, using the coordinate transformation method, we investigated the orientation dependences of elastic constants and engineering elastic parameters including Young's modulus, Possion's ratio, and the rigidity modulus of *mm*2 $Ca_3Mn_2O_7$. Orientations were specified along which the

†Corresponding author. E-mail: gjian@just.edu.cn
‡Corresponding author. E-mail: chaoyan@just.edu.cn

© 2019 Chinese Physical Society and IOP Publishing Ltd

maximum and minimum of these parameters can be obtained. The results reveal elastic parameters and magnetoelectric coefficients can be increased along specific orientations in *mm*2 point group orthorhombic $Ca_3Mn_2O_7$.

2. Methods

$Ca_3Mn_2O_7$ crystal below Neel temperature is a member of orthorhombic system with a point group of *mm*2. For space groups of $Cmc2_1$ and $A2_1am$, they exhibit almost the same crystal structures (Fig. 1).[7,28] The spontaneous polarization axis is along the *c* axis. $Ca_3Mn_2O_7$ crystal has two mirrors orthogonal with each other and one twofold axis. *a* and *b* axes of orthorhombic $Ca_3Mn_2O_7$ crystals are the normal lines of the two mirrors and the *c* axis is the twofold axis, respectively. Because $\alpha=\beta=\gamma=90^\circ$ applies to orthorhombic $Ca_3Mn_2O_7$ crystals, we choose an original crystallographic coordinate system along principle crystal axes of the $Ca_3Mn_2O_7$ cells for transformations, which is $X \parallel a$, $Y \parallel b$, $Z \parallel c$ (Fig. 1).

Two-step rotations were used to reach a desired arbitrary direction from the original coordinate system. First, a rotation through a clockwise angle ϕ about the Z axis makes original coordinates XYZ changed to new coordinates $X'Y'Z'$ ($Z' \parallel Z$).

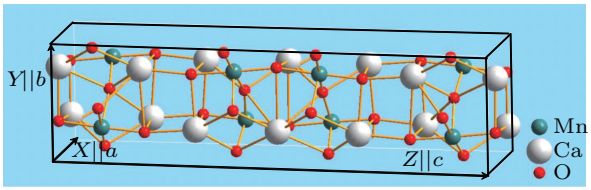


Fig. 1. Schematic illustration of $Ca_3Mn_2O_7$ crystal structure (orthorhombic system). The coordinate system (XYZ) of the crystal is chosen along principle crystal axes of the $Ca_3Mn_2O_7$ unit cell. Lattice constants: $\alpha=\beta=\gamma=90^\circ$, $c=1.944$ nm, $a=0.524$ nm, $b=0.525$ nm ($Cmc2_1$),[7] $\alpha=\beta=\gamma=90^\circ$, $c=1.942$ nm, $a=0.523$ nm, $b=0.524$ nm ($A2_1am$).[28]

The transformation matrix A_Z of this rotation is

$$A_Z=\begin{pmatrix}\cos\phi & \sin\phi & 0\\ -\sin\phi & \cos\phi & 0\\ 0 & 0 & 1\end{pmatrix}. \tag{1}$$

Second, a rotation through a clockwise angle θ about the X' axis makes the coordinate system $X'Y'Z'$ changed to another new coordinates $X''Y''Z''$ ($X'' \parallel X'$). The transformation matrix A_X of this rotation is

$$A_X=\begin{pmatrix}1 & 0 & 0\\ 0 & \cos\theta & \sin\theta\\ 0 & -\sin\theta & \cos\theta\end{pmatrix}. \tag{2}$$

N and M are $[6\times6]$ transformation matrices for stress. As a_{ij} represents the element in row i and column j in transformation matrix A, the relation between matrices M and N and A is

$$N=\begin{pmatrix}
a_{11}^2 & a_{12}^2 & a_{13}^2 & a_{12}a_{13} & a_{13}a_{11} & a_{11}a_{12}\\
a_{21}^2 & a_{22}^2 & a_{23}^2 & a_{22}a_{23} & a_{23}a_{21} & a_{21}a_{22}\\
a_{31}^2 & a_{32}^2 & a_{33}^2 & a_{32}a_{33} & a_{33}a_{31} & a_{31}a_{32}\\
2a_{21}a_{31} & 2a_{22}a_{32} & 2a_{23}a_{33} & a_{22}a_{33}+a_{32}a_{23} & a_{23}a_{31}+a_{33}a_{21} & a_{21}a_{32}+a_{31}a_{22}\\
2a_{31}a_{11} & 2a_{32}a_{12} & 2a_{33}a_{13} & a_{32}a_{13}+a_{12}a_{33} & a_{33}a_{11}+a_{13}a_{31} & a_{31}a_{12}+a_{11}a_{32}\\
2a_{11}a_{21} & 2a_{12}a_{22} & 2a_{13}a_{23} & a_{12}a_{23}+a_{22}a_{13} & a_{13}a_{21}+a_{23}a_{11} & a_{11}a_{22}+a_{21}a_{12}
\end{pmatrix}, \tag{3}$$

$$M=\begin{pmatrix}
a_{11}^2 & a_{12}^2 & a_{13}^2 & 2a_{12}a_{13} & 2a_{11}a_{13} & 2a_{11}a_{12}\\
a_{21}^2 & a_{22}^2 & a_{23}^2 & 2a_{22}a_{23} & 2a_{21}a_{23} & 2a_{21}a_{22}\\
a_{31}^2 & a_{32}^2 & a_{33}^2 & 2a_{32}a_{33} & 2a_{31}a_{33} & 2a_{31}a_{32}\\
a_{21}a_{31} & a_{22}a_{32} & a_{23}a_{33} & a_{22}a_{33}+a_{32}a_{23} & a_{23}a_{31}+a_{33}a_{21} & a_{21}a_{32}+a_{31}a_{22}\\
a_{11}a_{31} & a_{12}a_{32} & a_{13}a_{33} & a_{32}a_{13}+a_{12}a_{33} & a_{33}a_{11}+a_{13}a_{31} & a_{31}a_{12}+a_{11}a_{32}\\
a_{11}a_{21} & a_{12}a_{22} & a_{13}a_{23} & a_{12}a_{23}+a_{22}a_{13} & a_{13}a_{21}+a_{23}a_{11} & a_{11}a_{22}+a_{21}a_{12}
\end{pmatrix}. \tag{4}$$

For a three-dimensional space coordinate system, all physical quantities are presented in the form of matrices. The matrices of elastic stiffness (compliance) are $[6\times6]$-rank tensors. According to Euler's law of rotations, the physical quantity matrices in a new direction are calculated from

$$c'=M_X\cdot M_Z\cdot c\cdot M_Z^{\mathrm{T}}\cdot M_X^{\mathrm{T}}, \tag{5}$$

$$s'=N_X\cdot N_Z\cdot s\cdot N_Z^{\mathrm{T}}\cdot N_X^{\mathrm{T}}. \tag{6}$$

The symbol '′' represents a new matrix in a rotating coordinate system. The symbol 'T' denotes a transpose matrix. The orientation dependences of Young's modulus E, Possion's ratio v, and the rigidity modulus G were obtained from that of elastic compliances s_{11} and s_{12} and following equations

$$E'=1/s'_{11}, \tag{7}$$

$$v'=-s'_{12}/s'_{11}, \tag{8}$$

$$G'=-E'/2\left(1+v'\right). \tag{9}$$

The key to Eqs. (5)–(9) is using the correct original matrices that vary under different symmetry conditions. For orthorhombic $Ca_3Mn_2O_7$ (point group: *mm*2), the original matrix for

elastic constants c can be found in Ref. [29].

$$c = \begin{pmatrix} c_{11} & c_{12} & c_{13} & 0 & 0 & 0 \\ c_{12} & c_{22} & c_{23} & 0 & 0 & 0 \\ c_{13} & c_{23} & c_{33} & 0 & 0 & 0 \\ 0 & 0 & 0 & c_{44} & 0 & 0 \\ 0 & 0 & 0 & 0 & c_{55} & 0 \\ 0 & 0 & 0 & 0 & 0 & c_{66} \end{pmatrix}. \quad (10)$$

The limited terms in value (nine independent elastic constants) in Eq. (10) are decided by Newman's principle in the symmetry conditions *mm*2 point group.[24] The original matrix for elastic compliance is in the same form with Eq. (10). The values of parameters required to obtain c'_{ij}, E', ν', and G' of orthorhombic $Ca_3Mn_2O_7$ were summarized and re-calculated in Table 1.[19]

Table 1. Elastic stiffness c_{ij} (GPa) and compliance s_{ij} (10^{-12} m^2/N) of O-phase $Ca_3Mn_2O_7$. The values of s_{ij} were re-calculated from c_{ij} using an inverse matrix operation $(s) = (c)^{-1}$.

c_{11}	c_{12}	c_{13}	c_{22}	c_{23}	c_{33}	c_{44}	c_{55}	c_{66}
245	127	110	223	95	210	98	85	84
s_{11}	s_{12}	s_{13}	s_{22}	s_{23}	s_{33}	s_{44}	s_{55}	s_{66}
6.5	–2.8	–2.1	6.7	–1.6	6.6	10.2	11.8	11.9

Three-dimensional (3D) and two-dimensional (2D) representation graphs were drawn using commercial mathematical software Maple 18.

3. Results and discussion

The orientation dependences were calculated using transformation law in Eqs. (5)–(9) and original matrices in Eq. (10). The results are shown by means of 3D and 2D representation graphs. These graphs can be understood that the distance between a point in the graphs and the origin point represents the absolute value of the relative physical quantity in the new direction.

Figure 2(a) shows the orientation dependence of elastic constant c_{11} of orthorhombic $Ca_3Mn_2O_7$ crystal in the 3D space. It was drawn using the nine independent c_{ij} on $Ca_3Mn_2O_7$ as shown in Table 1. From Fig. 2(a), it can be found that elastic constant c'_{11} shows moderate orientation dependences along different orientations. c'_{11} shows evident changes at the first rotation about the Z axis at angles ϕ. The min $c'_{11} = 245$ GPa can be found at $\phi = 0°$ and 90°, while the max $c'_{11} = 265.6$ GPa is obtained at $\phi = 45°$ (also see the 2D cross-sectional plot in Fig. 2(b)). A difference of $\Delta c'_{11} = 20.5$ GPa which is 7.7% of the max c_{11} indicating moderate changes.

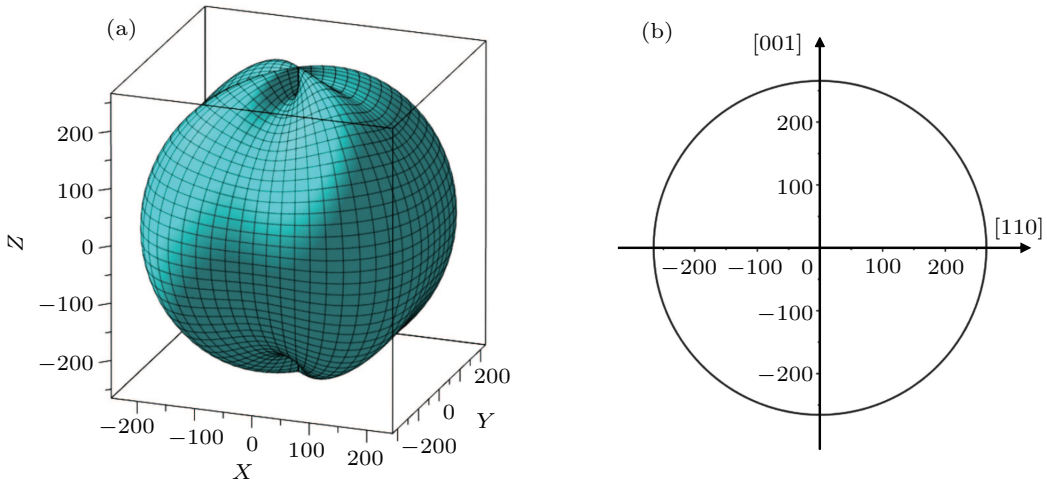


Fig. 2. (a) Schematic diagram of elastic constant c_{11} of orthorhombic $Ca_3Mn_2O_7$, (b) elastic constant c_{11} of orthorhombic $Ca_3Mn_2O_7$ in $X'OZ$ plane ($\phi = 45°$, unit GPa).

Figure 3(a) shows the orientation dependence of elastic constant c_{12} of $Ca_3Mn_2O_7$ crystal in the 3D space. From Fig. 3(a), it can be found that elastic constant c'_{12} shows larger orientation dependences than c'_{11}. c'_{12} changes at both of the two rotations at different ϕ and θ. When the coordinate system rotates about Z axis at $\theta = 90°$ and $\theta = 90°$ ($Ca_3Mn_2O_7 \parallel [010]$), c'_{12} tends to be small (the min $c'_{12} = 95$ GPa). A 2D cross-section plot (an ellipse) in Fig. 3(b) shows that the max $c'_{12} = 127$ GPa is obtained at $\theta = 0°$, *i.e.*, along the Z axis ($Ca_3Mn_2O_7 \parallel [001]$).

Because at the atomic scale, applying the Harshe model for strong electromaechanical and megnetomechanical interactions in single-phase magnetoelectric compounds, magnetoelectric coefficients α_{E31} (transverse) and α_{E33} (longitudinal) are increasing with decreasing $c_{11} + c_{12}$.[23,24] And from the above results of anisotropy of elastic constants $c_{11} + c_{12}$, which have a min value along [nk0] direction and a max value along [001] direction. Thus, magnetoelectric coefficients α_{E31} and α_{E33} may have an increased value along [nk0] directions for the increased elastic transport abilities, while both α_{E31} and α_{E33} tend to be decreased values along [001] direction for the compressed elastic transport abilities.

Figure 4(a) shows the orientation dependence of elastic constant c_{13} of $Ca_3Mn_2O_7$ crystal in the 3D space. From the geometry in Fig. 4(a), the min $c'_{13} = 96$ GPa exists at orientations summarized as $\phi = 45°$, the max $c'_{13} = 127$ GPa can be obtained along [100] and [010] axes. Figure 4(b) shows a 2D cross-section plot of c'_{13} in XOZ or YOZ planes, besides the orientation of the max c'_{13} can be confirmed, $c'_{13} = 110$ GPa along [001] also can be observed.

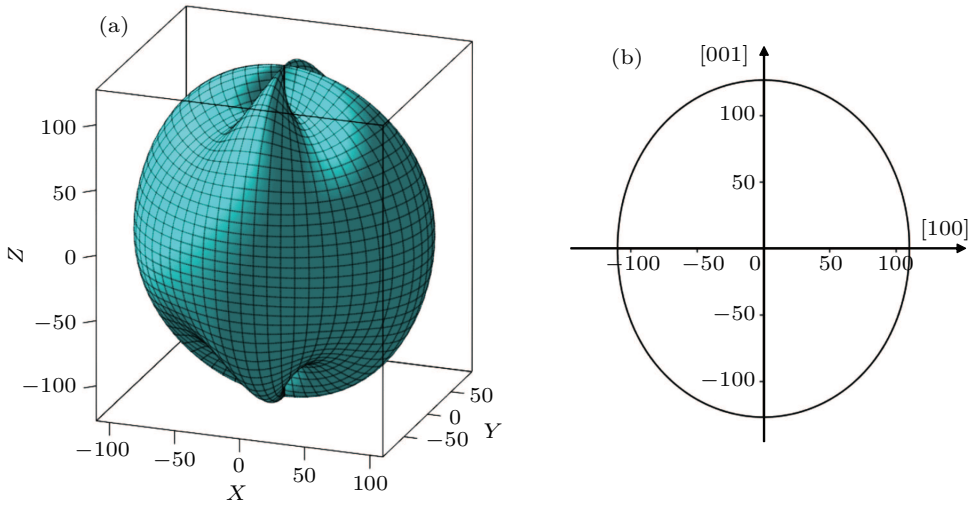


Fig. 3. (a) Schematic diagram of elastic constant c_{12} of orthorhombic $Ca_3Mn_2O_7$, (b) elastic constant c_{12} of orthorhombic $Ca_3Mn_2O_7$ in XOZ plane (unit GPa).

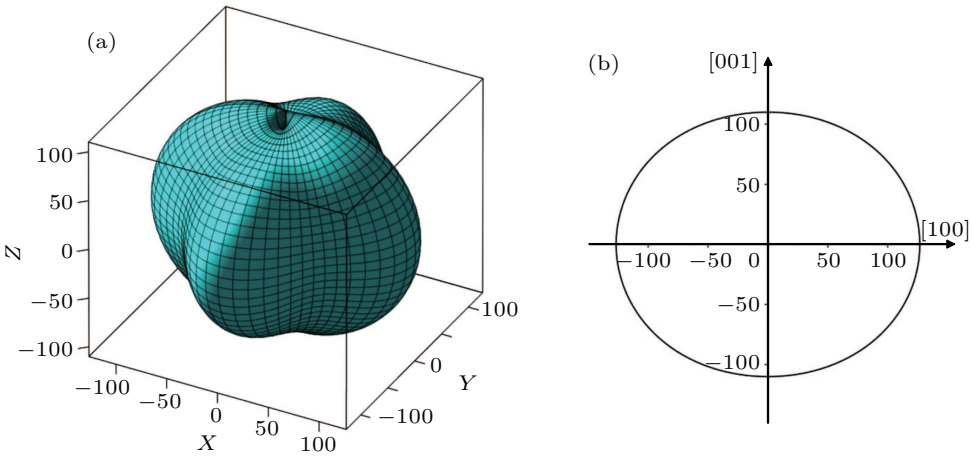


Fig. 4. (a) Schematic diagram of elastic constant c_{13} of orthorhombic $Ca_3Mn_2O_7$, (b) elastic constant c_{13} of orthorhombic $Ca_3Mn_2O_7$ in XOZ plane (also applied to YOZ plane, unit GPa).

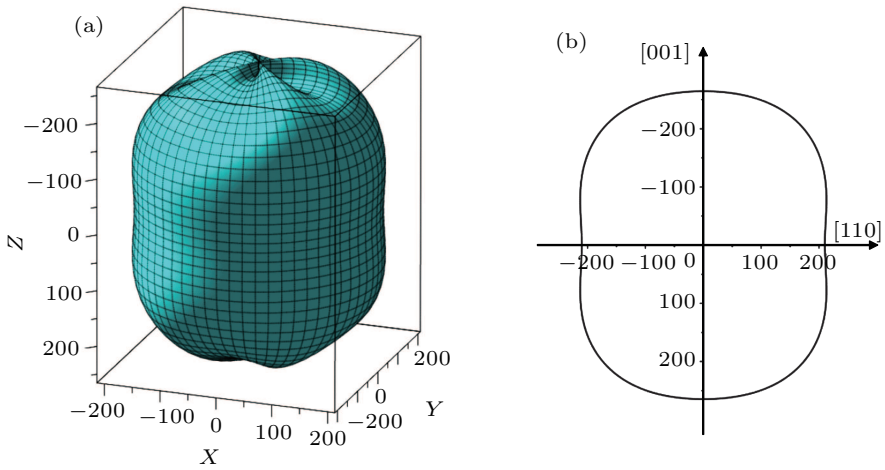


Fig. 5. (a) Schematic diagram of elastic constant c_{22} of orthorhombic $Ca_3Mn_2O_7$, (b) elastic constant c_{22} of orthorhombic $Ca_3Mn_2O_7$ in $X'OZ$ plane ($\phi = 45°$, unit GPa).

Figure 5(a) shows the orientation dependence of elastic constant c_{22} of $Ca_3Mn_2O_7$ crystal in the 3D space. From the geometry in Fig. 5(a), it has a shape like a cylinder. Large c'_{22} exist at small θ angles apart from the Z axis. The max $c'_{22} = 265.6$ GPa is obtained at $\theta = 0^\circ$ and $\phi = 45^\circ$, also see a 2D cross-section plot in $X'OZ$ plane ($\phi = 45^\circ$) in Fig. 5(b). The min $c'_{22} = 96$ GPa can be found along orientations summarized as $\theta = 90^\circ$ ($Ca_3Mn_2O_7 \perp [001]$).

Figure 6(a) shows the orientation dependence of elastic constant c_{33} of $Ca_3Mn_2O_7$ crystal in the 3D space. The geometry of c'_{33} is near a cubic but with very flat angles. The min $c'_{33} = 213$ GPa exist along the main crystalline axes of $Ca_3Mn_2O_7$, while the large c'_{33} exist at $\phi = 45^\circ$, and the max $c'_{33} = 265.6$ GPa is obtained at $\phi = 45^\circ$ and $0^\circ < \theta < 34^\circ$ (Fig. 6(b)).

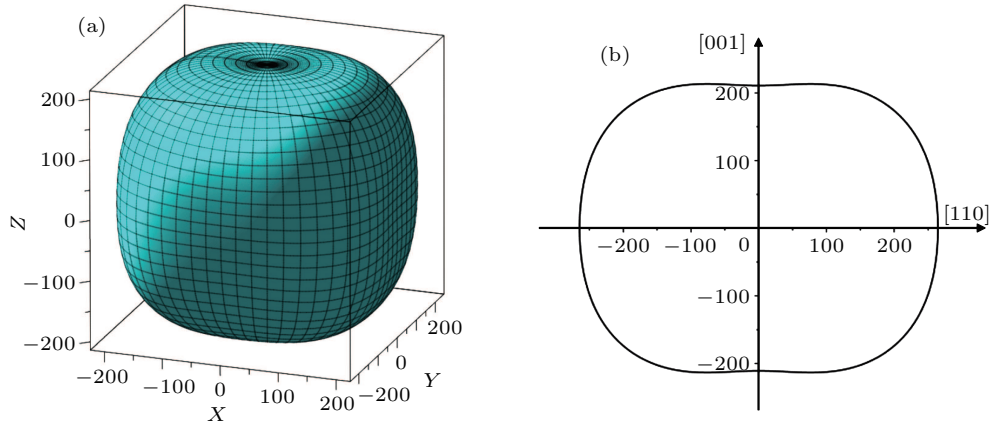


Fig. 6. (a) Schematic diagram of elastic constant c_{33} of orthorhombic $Ca_3Mn_2O_7$, (b) elastic constant c_{33} of orthorhombic $Ca_3Mn_2O_7$ in $X'OZ$ plane ($\phi = 45^\circ$, unit GPa).

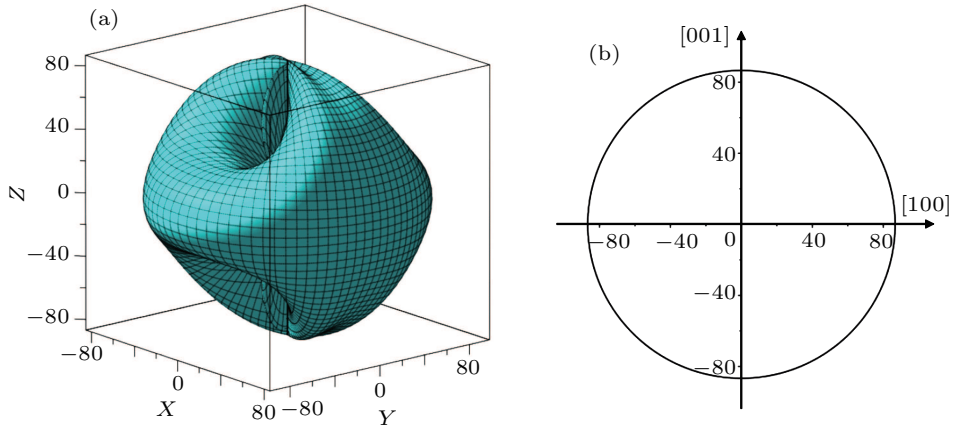


Fig. 7. (a) Schematic diagram of elastic constant c_{66} of orthorhombic $Ca_3Mn_2O_7$, (b) elastic constant c_{66} of orthorhombic $Ca_3Mn_2O_7$ in XOZ plane (also applies to XOY plane, unit GPa).

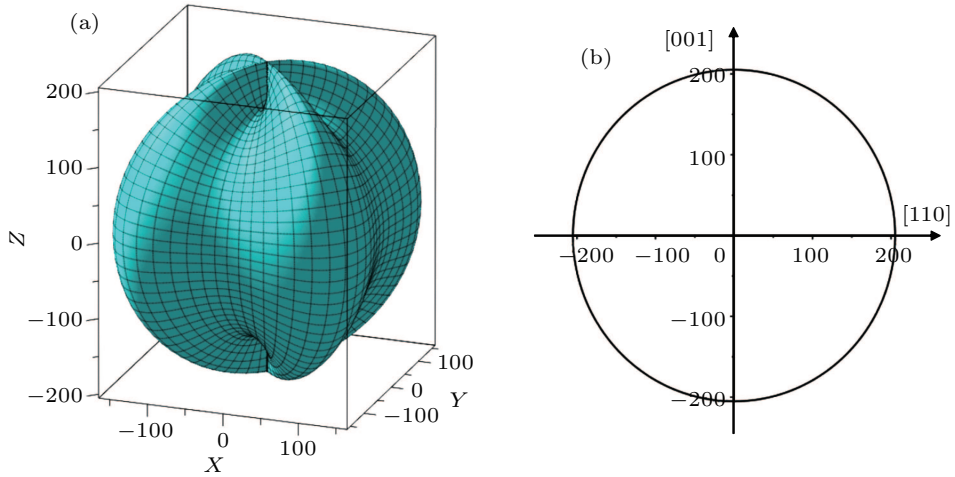


Fig. 8. (a) Schematic diagram of Young's modulus E of orthorhombic $Ca_3Mn_2O_7$, (b) Young's modulus E of orthorhombic $Ca_3Mn_2O_7$ in $X'OZ$ plane ($\phi = 45^\circ$, unit GPa).

Figure 7(a) shows the orientation dependence of elastic constant c_{66} of $Ca_3Mn_2O_7$ crystal in the 3D space. From Fig. 7(a), it can be found that, along three main crystalline axes, elastic constant c'_{66} all have the max value, which is 87 GPa. Along orientations at $\theta = 27°$ and $\phi = 90°$, c'_{66} tends to be very small close to zero. The 2D cross-section plot in XOZ plane in Fig. 7(b) also applies to XOY plane. The orientations where the max c'_{66} exist can be summarized as $\theta = 90°$ or $\phi = 0°$.

Figure 8(a) shows the orientation dependence of Young's modulus E (change in length per unit length for a tensile stress) of $Ca_3Mn_2O_7$ crystal in the 3D space. It was decided by using Eq. (7) and nine independent compliance s_{ij} on $Ca_3Mn_2O_7$ as shown in Table 1. From the geometry showed in Fig. 8(a), the Young's modulus E' shows evident orientation dependences during rotations. The min $E' = 154$ GPa exists at orientations summarized as $\phi = 0°$ and 90°. A 2D cross-section plot in Fig. 8(b) shows that the max $E' = 205$ GPa is obtained at $\phi = 45°$. It should be noted that, along three main crystal axes, the max E' exists along [001], while the min E' exists along [100] and [010].

Figure 9(a) shows the orientation dependence of Poisson's ratio v (the ratio of the transverse contraction to the longitudinal elongation) of $Ca_3Mn_2O_7$ crystal in the 3D space. It was determined by orientation dependences of compliances s'_{11} and s'_{12} and Eq. (8). From Fig. 9(a), it can be found that Poisson's ratio v' shows strong orientation dependences along different orientations. The min v' tends to zero exist along [100] axis. A 2D cross-section plot in Fig. 9(b) shows that the max absolute $v' = 0.657$ is obtained at along [001] axis. $v' = 0.23$ along [010] axis also can be found from Fig. 9(b).

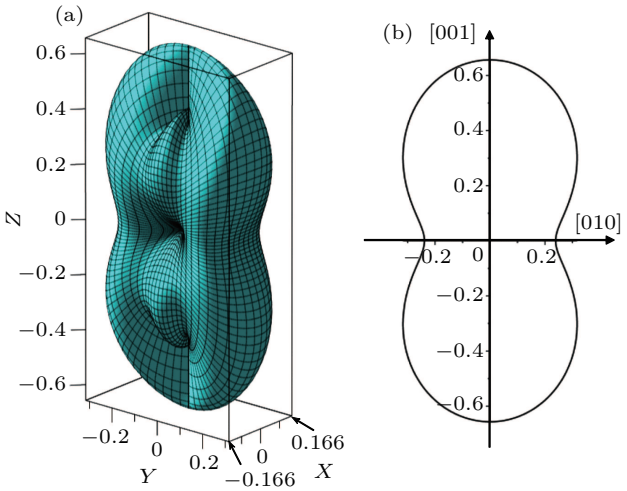


Fig. 9. (a) Schematic diagram of Poisson's ratio v by of orthorhombic $Ca_3Mn_2O_7$, (b) Poisson's ratio v of orthorhombic $Ca_3Mn_2O_7$ in YOZ plane.

Figure 10(a) shows the orientation dependence of the rigidity modulus G (a measure of shear strain under shear stress) of $Ca_3Mn_2O_7$ crystal in the 3D space. It was determined by orientation dependences of E and v and Eq. (9). From the geometry in Fig. 10(a), it can be found that the rigidity modulus G' shows strong orientation dependences during rotations. The $G' = 77$ GPa along orientations summarized as $\phi = 0°$ and 90°. A 2D cross-section plot in Fig. 10(b) shows that the max $G' = 88$ GPa is obtained at $\phi = 45°$.

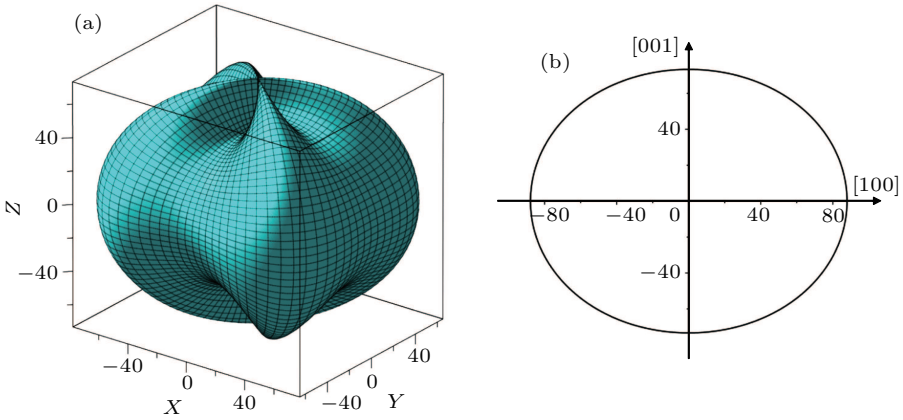


Fig. 10. (a) Schematic diagram of the rigidity modulus G of orthorhombic $Ca_3Mn_2O_7$, (b) the rigidity modulus G of orthorhombic $Ca_3Mn_2O_7$ in $X'OZ$ plane ($\phi = 45°$, unit GPa).

4. Conclusion

In this study, we investigated basic elastic parameters (elastic constants c'_{ij}) and engineering elastic parameters (Young's modulus E', Poisson's ratio v', and the rigidity modulus G') of orthorhombic $Ca_3Mn_2O_7$ (applying to both $Cmc2_1$ and $A2_1am$ space groups with a point group of $mm2$) along arbitrary orientations, and concluded the effects of elastic properties may have on the value of magnetoelectric coefficients. The max $c'_{11} = c'_{33} = 265.6$ GPa, $E' = 205$ GPa, and $G' = 88$ GPa are obtained along orientation clusters at $\phi = 45°$, the max $c'_{66} = 87$ GPa is obtained along orientation clusters at $\theta = 90°$ or $\phi = 0°$, the max $c'_{12} = 127$ GPa, $c'_{22} = 265.6$ GPa, and $v' = 0.657$ are obtained along [001] axis, the max $c'_{13} = 127$ GPa is obtained along [100] or [010] axes, respectively. Both α_{E31} and α_{E33} may have an increased value along $[nk0]$ for the increased elastic transport abilities, while

both α_{E31} and α_{E33} tend to be decreased value along [001] for the compressed elastic transport abilities. The results reveal elastic parameters and magnetoelectric coefficients can be increased along specific orientations in *mm*2 point group orthorhombic $Ca_3Mn_2O_7$.

References

[1] Fishman R S 2013 *Phys. Rev. B* **87** 224419

[2] Shimamoto K, Mukherjee S, Manz S, White J S, Trassin M, Kenzelmann M, Chapon L, Lippert T, Fiebig M, Schneider C W and Niedermayer C 2017 *Sci. Rep.* **7** 44753

[3] Kimura T, Tomioka Y, Kuwahara H, Asamitsu A, Tamura M and Tokura Y 1996 *Science* **274** 1698

[4] Benedek N A and Fennie C J 2011 *Phys. Rev. Lett.* **106** 107204

[5] Zhu W, Pi L, Huang Y, Tan S and Zhang Y 2012 *Appl. Phys. Lett.* **101** 192407

[6] Bendersky L A, Greenblatt M and Chen R 2003 *J. Solid State Chem.* **174** 418

[7] Lobanov M V, Greenblatt M, Caspi E N, Jorgensen J D, Sheptyakov D V, Toby B H, Botez C E and Stephens P W 2004 *J. Phys.: Condens. Matter* **16** 5339

[8] Senn M S, Bombardi A, Murray C A, Vecchini C, Scherillo A, Luo X and Cheong S W 2015 *Phys. Rev. Lett.* **114** 035701

[9] Lee M H, Chang C P, Huang F T, Guo G Y, Gao B, Chen C H, Cheong S W and Chu M W 2017 *Phys. Rev. Lett.* **119** 157601

[10] Gao B, Huang F T, Wang Y, Kim J W, Wang L, Lim S J and Cheong S W 2017 *Appl. Phys. Lett.* **110** 222906

[11] Glamazda A, Wulferding D, Lemmens P, Gao B, Cheong S W and Choi K Y 2018 *Phys. Rev. B* **97** 094104

[12] Dewhurst J K, Sharma S and Nordstrom L 2009 *Spacegroup Manual* Version 1.1.4 (CEST), pp. 4–14

[13] Conway J H, Olaf D F, Huson D H and Thurston W P 2001 *Beiträge Zur Algebra Und Geometrie. Contributions to Algebra and Geometry* **42** 475

[14] Liu M, Zhang Y, Lin L F, Lin L, Yang S, Li X, Wang Y, Li S, Yan Z, Wang X, Li X G, Dong S and Liu J M 2018 *Appl. Phys. Lett.* **113** 022902

[15] Matar S F, Eyert V, Villesuzanne A and Whangbo M H 2007 *Phys. Rev. B* **76** 054403

[16] Maccheshev J B, Williams H J, Sherwood R C and Potter J F 1968 *J. Appl. Phys.* **39** 1206

[17] Harris A B 2011 *Phys. Rev. B* **84** 064116

[18] Shen J Y, Johnston S, Shang S L and Anderson T 2002 *J. Crystal Growth* **240** 6

[19] Zhang W and Tong P Q 2013 *Chin. Phys. B* **22** 066201

[20] Huang H, Ma X, Liu Z and Ma X 2018 *Chin. Phys. B* **27** 016201

[21] Yan P, Chong X Y, Jiang Y H and Feng J 2017 *Chin. Phys. B* **26** 126202

[22] Nan C W, Bichurin M I, Dong S, Viehl, D and Srinivasan G 2008 *J. Appl. Phys.* **103** 031101

[23] Kumar A, Scott J F, Martinez R, Srinivasan G and Katiyar R S 2012 *Phys. Status Solidi A* **209** 1207

[24] Singh M K, Prellier W, Singh M P, Katiyar R S and Scott J F 2008 *Phys. Rev. B* **77** 144403

[25] Du X, Wang Q, Belegundu U, Bhalla A and Uchino K 1999 *Mater. Lett.* **40** 109

[26] Yue W and Jian J Y 2003 *Opt. Mater.* **23** 403

[27] Jian G, Xue F, Zhang C, Yan C, Zhao N and Wong C P 2017 *J. Magn. Magn. Mater.* **442** 141

[28] Guiblin N, Grebille D, Leligny H and Martin C 2002 *Acta Crystallogr C* **58** i3

[29] Newnham R E 2005 *Properties of Materials. Anisotropy, Symmetry, Structure* (Oxford: Oxford University Press), pp. 108–109